

Word4Per: Zero-shot Composed Person Retrieval

Delong Liu, Haiwen Li, Zhicheng Zhao, *Member, IEEE*, Fei Su, *Member, IEEE*, Yuan Dong

Abstract—Searching for specific person has great social benefits and security value, and it often involves a combination of visual and textual information. Conventional person retrieval methods, whether image-based or text-based, usually fall short in effectively harnessing both types of information, leading to the loss of accuracy. In this paper, a whole new task called Composed Person Retrieval (CPR) is proposed to jointly utilize both image and text information for target person retrieval. However, the supervised CPR requires very costly manual annotation dataset, while there are currently no available resources. To mitigate this issue, we firstly introduce the Zero-shot Composed Person Retrieval (ZS-CPR), which leverages existing domain-related data to resolve the CPR problem without expensive annotations. Secondly, to learn ZS-CPR model, we propose a two-stage learning framework, Word4Per, where a lightweight Textual Inversion Network (TINet) and a text-based person retrieval model based on fine-tuned Contrastive Language-Image Pre-training (CLIP) network are learned without utilizing any CPR data. Thirdly, a finely annotated Image-Text Composed Person Retrieval (ITCPR) dataset is built as the benchmark to assess the performance of the proposed Word4Per framework. Extensive experiments under both Rank-1 and mAP demonstrate the effectiveness of Word4Per for the ZS-CPR task, surpassing the comparative methods by over 10%. The codes and ITCPR dataset will be made publicly available at <https://github.com/Delong-liu-bupt/Word4Per>.

Index Terms—Zero-shot, Composed Person Retrieval, ITCPR Dataset, Textual Inversion Network

I. INTRODUCTION

Person retrieval [1], [2] aims to identify target person images from a large-scale person gallery. It comprises two popular directions: Image-based Person Retrieval (IPR) [3] and Text-based Person Retrieval (TPR) [4], which are dedicated to using images and texts commonly acquired in daily life as queries to identify the targets of interest. In recent years, due to its extensive applications in social services and public security, person retrieval has garnered increasing attention.

In real scenarios, when seeking a specific person, both visual and textual information are often available, while IPR and TPR methods can not fully leverage all information, inevitably leading to a certain loss in accuracy. Therefore, as shown in Fig. 1, we propose a novel task, Composed Person Retrieval (CPR), to simultaneously utilize visual and textual information for retrieving the target person. The CPR task is a variant of the Composed Image Retrieval (CIR) task [5], where the dataset consists of a large number of triplets (I_q, T_q, I_t) , comprising a reference image (I_q) , a relative caption (T_q) , and several target images (I_t) . This type of data is manually collected and annotated and this process is time-consuming and expensive.

Delong Liu, Haiwen Li, Zhicheng Zhao, Fei Su and Yuan Dong are with the Beijing University of Posts and Telecommunications, and Zhicheng Zhao, Fei Su and Yuan Dong are also with the Beijing Key Laboratory of Network System and Network Culture, Beijing, China (e-mail: liudelong@bupt.edu.cn; lihuiwen52@bupt.edu.cn; zhaozc@bupt.edu.cn; sufei@bupt.edu.cn; yuandong@bupt.edu.cn). (Corresponding author: Zhicheng Zhao.)

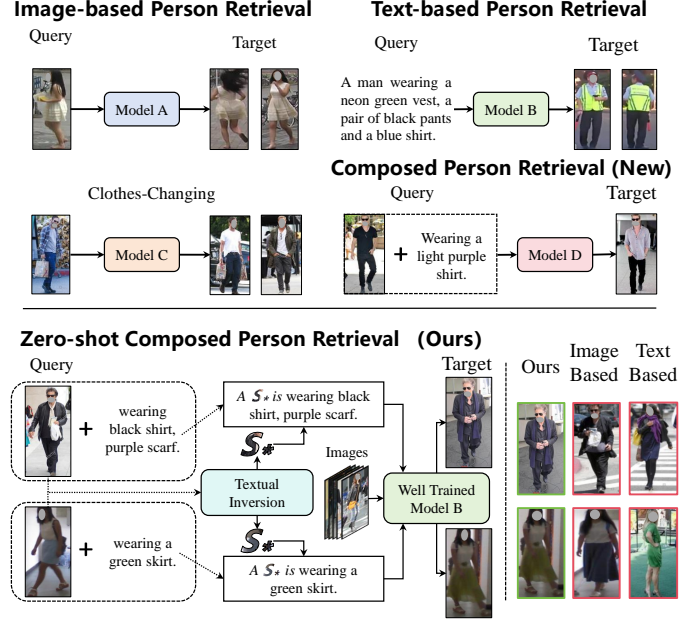


Fig. 1. Existing methods and our proposed new task. **Top:** IPR aims to train a model (*Model A* and *Model C*) to identify the target person using a reference image, while TPR models (*Model B*) find the target person using text. Our proposed CPR task aims to learn a model (*Model D*) to identify the target by combining visual and textual information. **Bottom:** To avoid using of costly triplets data to train *Model D*, we introduce the ZS-CPR task and propose a solution: Word4Per.

Moreover, previous research [5], [6] in the CIR field has shown that training a fully supervised network (*Model D*) heavily depends on large-scale dataset, which is not available for the CPR task.

To address this challenge, we introduce a new task named as Zero-shot Composed Person Retrieval (ZS-CPR), aiming to present a new method that no longer relies on costly triplet annotations for supervised learning but rather uses existing image-text data to solve the CPR issue. And correspondingly, a two-stage framework called Word4Per is proposed to learn the ZS-CPR model, where image-text datasets [4], [7], [8] for the TPR task are utilized. Specifically, in the first stage, we introduce a cross-modal retrieval network to maximize the similarity between person images and their captions. In the second stage, a lightweight Textual Inversion Network (TINet) is constructed to map the image into a special word. By this way, a flexible combination of reference image and relative caption for retrieval can be obtained. Furthermore, for effective evaluation the performance of Word4Per method, a test set ITCPR is constructed via reusing public person retrieval datasets such as Celeb-reID [9], LAST [10], and PRCC [11]. Annotating the relative captions is achieved by selecting images of the same identity with different outfits,

and finally, a complete set of triplets is created.

As shown in Fig. 1, in practical applications, the trained TINet is used to transform the reference image I_q into a pseudo-word S_* . Subsequently, this pseudo-word is concatenated via using a sentence template with the relative caption T_q . The well-trained *Model B* is then used for person retrieval, finding the corresponding targets.

To validate the effectiveness of our proposed the Word4Per framework and ITCPR dataset for the ZS-CPR task, extensive experiments are conducted. The experimental results show significant improvements in evaluation metrics compared to the state-of-the-art methods [12], [2]. The main contributions can be summarized as follows:

- A novel cross-modal task, named zero-shot composed person retrieval, is proposed to deal with the CPR problem without costly triplet annotations.
- We propose an efficient and flexible Word4Per framework for ZS-CPR, in which a lightweight textual inversion network and a TPR model are learned without utilizing any CPR triplets data.
- We annotate and build a new ITCPR dataset for the ZS-CPR task.
- Extensive experiments validate the effectiveness of our proposed Word4Per framework and ITCPR dataset.

II. RELATED WORK

A. Person Retrieval

Person retrieval consists of two main branches: IPR and TPR. IPR, the older subfield, has witnessed extensive research on feature extraction [3], [13], [14], metric learning [15], lightweight models [16], [17], [18], multi-branch methods [19], [1], [20], and attention mechanisms [21], [22]. Recently, transformer-based models like PAT [23], DRL-Net [24], and TransReID [25] have gained popularity by combining ResNet-50 [26] with Transformer [27] decoders, achieving outstanding performance on large datasets. A recent popular variant of the IPR task is clothes-changing person retrieval [9], aimed at finding the same person with different clothing. This field has given rise to a plethora of datasets [9], [11], [10] and works [28], [29], [30].

In contrast, TPR [4], [31], [32] is a relatively younger field, but it has progressed rapidly thanks to the development of text-image pre-training models [12], [33]. TPR aims to align image and text features in a shared embedding space to facilitate person matching. Early TPR methods [34], [35] primarily focus on extracting global [35] and local features [36], [34] from image-text pairs and then using matching loss for modality alignment. However, they often struggle to balance efficiency and performance. Recent research [2], [37], [38] has introduced auxiliary tasks to enable implicit feature alignment, thereby enhancing performance without increasing inference complexity. In [2], [39], the pre-trained language-image model (CLIP) [12] is directly applied to TPR, and through fine-tuning, it achieves outstanding TPR performance.

However, despite these advancements, the aforementioned methods still struggle to effectively integrate textual and visual information to identify the target person, which remains a common and critical application.

B. Composed Image Retrieval

Composed Image Retrieval (CIR) [6], [5], [40] aims to achieve diverse image retrieval by merging image and text queries. This task belongs to the broader field of compositional learning [41], [42] and has been explored in various domains like fashion [43], [44] and scene composition [45], booming different fusion and training techniques. For instance, self-training shallow Transformers [27] and pre-trained Bert [46] models are utilized to fuse images and texts. However, these methods typically require training on carefully annotated CIR datasets [44], [45] and only perform effectively on images related to the training set. Consequently, the Zero-Shot Composed Image Retrieval (ZS-CIR) [47], [48] has been introduced. They leverage the powerful modality alignment capabilities of big models like CLIP to convert image information into pseudo-text information [49], enabling the completion of the task without CIR datasets. Compared with Composed Image Retrieval (CIR), the CPR task concentrates more on subtle changes and is more challenging. Therefore, our method differs from that described in [47], [48], which focuses exclusively on text reversal without attempting to fine-tune the text-image retrieval models. Specifically, Pic2Word [47] only uses images during training, leading to the inversion network that fails to effectively focus on the main subjects, and requires a large amount of training data to demonstrate its zero-shot capability. Additionally, the inversion process in SEARLE [48] involves interventions by LLMs, and is therefore a multi-stage and resource-intensive operation. In contrast, our text inversion network can be trained end-to-end, offering greater efficiency. Additionally, it leverages semantic information to direct the inversion network's attention to the main subjects, thereby effectively handling the CPR task.

III. METHOD

The proposed Word4Per framework, shown in Fig. 2, consists of two main parts: fine-tuning the CLIP network (Section III-A) and learning a TINet (Section III-B). Firstly, three supervised losses are adopted to align visual-textual features via fine-tuning CLIP. Then, a lightweight TINet is built to optimize the transformation of visual information into pseudo-words. During inference (Section III-C), the trained TINet generates pseudo-word tokens, which are inserted into a sentence template with the caption and fed into the text encoder to produce the final text features for person retrieval.

A. Fine-tuning of CLIP Network

1) *Rationale for Fine-Tuning*: In consideration of the fact that CLIP's pretraining data is not specifically tailored for person retrieval, we fine-tune it using person-specific image-text data. This fine-tuning addresses identity issues and fine-grained details in person descriptions through two losses: a similarity distribution matching loss \mathcal{L}_{sdm} [2], which aligns the feature representations of different modalities for the same identity, and an identity (ID) loss \mathcal{L}_{id} [35], which ensures that features within the same modality for the same identity are brought closer together.

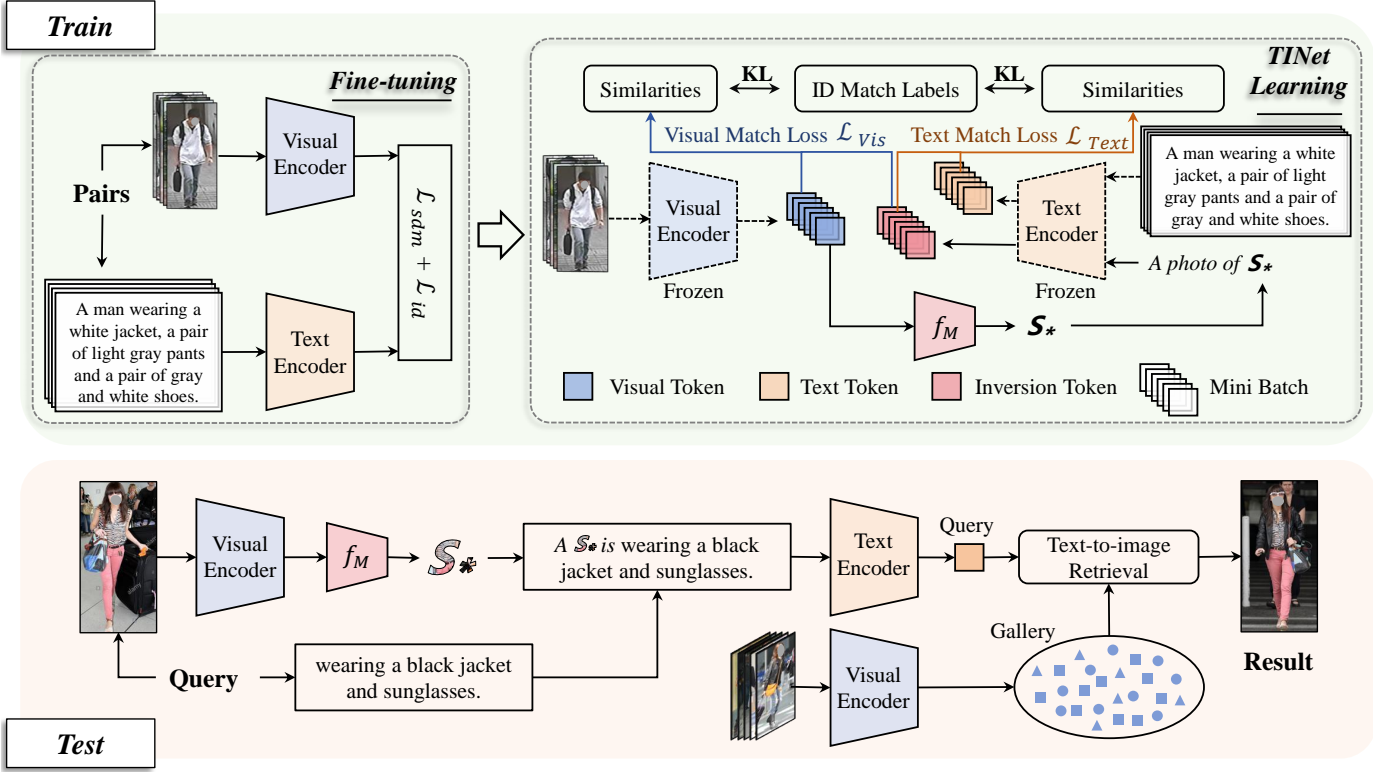


Fig. 2. Training and inference of the Word4Per framework. **Top:** The training process is divided into two stages, and the first one is the fine-tuning phase, in which two losses (\mathcal{L}_{sdm} , \mathcal{L}_{id}) are used to optimize the visual and text encoders. The second stage is the training of the TINet f_M , where two contrastive learning losses \mathcal{L}_{vis} and \mathcal{L}_{text} are applied to supervise the generation of pseudo-word S_* . **Bottom:** During the testing phase, the well-trained dual encoders and TINet are used to accomplish CPR task.

2) *Similarity Distribution Matching Loss and Identity Loss:* Aiming to match feature representations between different modalities, a cross-modal projection matching loss \mathcal{L}_{sdm} is adopted. \mathcal{L}_{sdm} utilizes cosine similarity distributions to compute matching probabilities for $N \times N$ image-text pairs within a mini batch and employs KL divergence to measure the difference between these probabilities and the true matching labels. For each global embedding f_i^v of an image, we can create a set of image-text embedding pairs $\{(f_i^v, f_j^t), l_{i,j}\}_{j=1}^N$, where $l_{i,j}$ is the true matching label. $l_{i,j} = 1$ indicates that (f_i^v, f_j^t) forms a matching pair from the same identity, while $l_{i,j} = 0$ denotes a non-matching pair. The cosine similarity between \mathbf{u} and \mathbf{v} , $\text{sim}(\mathbf{u}, \mathbf{v}) = \mathbf{u}^\top \mathbf{v} / \|\mathbf{u}\| \|\mathbf{v}\|$, is \mathcal{L}_2 normalized. The formula for calculating the matching probability is as follows:

$$p_{i,j} = \frac{\exp(\text{sim}(f_i^v, f_j^t) / \tau)}{\sum_{h=1}^N \exp(\text{sim}(f_i^v, f_h^t) / \tau)}, \quad (1)$$

where τ is a temperature hyperparameter controlling the peak of the probability distribution. Within a mini batch, the image-to-text matching loss is calculated using the following formula:

$$\mathcal{L}_{i2t} = KL(\mathbf{p}_i \| \mathbf{q}_i) = \frac{1}{N} \sum_{i=1}^N \sum_{j=1}^N p_{i,j} \log \left(\frac{p_{i,j}}{q_{i,j} + \epsilon} \right), \quad (2)$$

where ϵ is a small value to avoid numerical issues, and $q_{i,j} = l_{i,j} / \sum_{k=1}^N l_{i,k}$ represents the true matching probability.

Similarly, the text-to-image matching loss \mathcal{L}_{t2i} can be formalized by swapping f^v and f^t in equations (1) and (2),

and the bidirectional matching loss \mathcal{L}_{sdm} is calculated as follows:

$$\mathcal{L}_{sdm} = \mathcal{L}_{i2t} + \mathcal{L}_{t2i}. \quad (3)$$

Furthermore, to ensure that the feature representations of the same image/text pair are closely clustered together in the joint embedding space, a common ID loss (\mathcal{L}_{id}) is used to supervise the identity label.

3) *Overall Objective:* In summary, the overall optimization objective for the fine-tuning is:

$$\mathcal{L} = \mathcal{L}_{sdm} + \mathcal{L}_{id}. \quad (4)$$

B. Learning the Textual Inversion Network

1) *Design of TINet:* As mentioned before, TINet maps image information to the linguistic space, where both image and text information in CLIP are represented by one-dimensional fixed-length vectors. Therefore, the TINet offers highly lightweight choice, allowing the mapping to be completed with minimal optimization complexity and optimal implementation speed. Specifically, we use a shallow fully connected network that learns to map the global image representation f_i^v into a pseudo-word token based on image-text pairs. Since images and texts of the same identity are highly related, the loss function for TINet optimization incorporates identity information.

2) *Training Process of TINet*: As shown in the top of Fig. 2, after completing the fine-tuning of the dual encoders, the training of the TINet is conducted with the dual encoders fully frozen. For the same batch of N image-text pairs, it is still able to construct a set of image-text representation pairs $\{(f_i^v, f_j^t), l_{i,j}\}_{j=1}^N$, where $l_{i,j}$ represents the real matching labels. The global embedding f_i^v of each image is used to obtain pseudo-word embeddings as tokens $S_* = f_M(f_i^v)$. Subsequently, it is appended to the end of token embeddings of the prompt sentence, 'a photo of', resulting in \hat{S}_* . Then \hat{S}_* is fed into the text encoder to obtain textual inversion embedding $f_k^c, k = 1, 2, \dots, N$. Similarly, we obtain the set of embeddings for image and textual inversion pairs $\{(f_i^v, f_k^c), l_{i,k}\}_{k=1}^N$ and the corresponding set of text and textual inversion encoding pairs $\{(f_j^t, f_k^c), l_{j,k}\}_{k=1}^N$, where the real matching labels $l_{i,k}$ and $l_{j,k}$ are equal to the corresponding positions of $l_{i,j}$.

Through TINet, each pseudo-word embedding is expected to closely match the corresponding image. Therefore, the contrastive learning loss based on \mathcal{L}_{sdm} is introduced to achieve this objective, i.e.,

$$\begin{cases} \mathcal{L}_{Vis} = \mathcal{L}_{i2c} + \mathcal{L}_{c2i}, \\ \mathcal{L}_{Text} = \mathcal{L}_{t2c} + \mathcal{L}_{c2t}, \end{cases} \quad (5)$$

where \mathcal{L}_{i2c} is computed by replacing f^t with f^c in equations (1) and (2), \mathcal{L}_{c2i} is computed by replacing f^v with f^c and f^t with f^v , \mathcal{L}_{t2c} is computed by replacing f^v with f^t and f^t with f^c , and \mathcal{L}_{c2t} is computed by replacing f^v with f^c . The \mathcal{L}_{Vis} focuses more on visual information in the image, while the \mathcal{L}_{Text} focuses more on semantic information corresponding to the image.

3) *Importance of Fine-Tuning and TINet Training*: Fine-tuning of CLIP and training of TINet are crucial for the Word4Per to acquire the combined zero-shot retrieval capability. TINet's training relies on a highly aligned dual encoder, and the trained TINet can convert image information into pseudo-word that can be easily concatenated to sentences, thereby transforming the CPR task into a general TPR task implemented by fine-tuned CLIP.

C. Inference

During inference, a reference image with a relative caption is combined to find the target person among gallery images. As shown in the bottom of Fig. 2, the query consists of two parts: an image and a textual caption. The image query passes through the visual encoder and the TINet f_M sequentially to obtain the inverted word S_* . Then, the query information is concatenated by using a sentence template 'a $[S_*]$ is {Caption}', and finally, the concatenated sentence serves as a text query to search for the target image in the gallery.

D. Flexibility in Training and Testing.

Word4Per is flexible in both training and testing. As shown in Fig. 3, multiple TINets (f_M) can be trained simultaneously with consistent input data, each configured flexibly in structure and loss functions. With the visual and text encoders frozen,

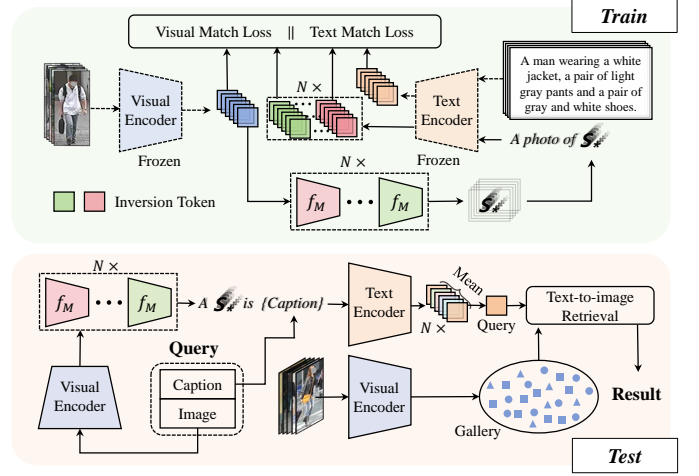


Fig. 3. Flexibility in Training and Inference. **Top**: The flexibility of the TINet training process allows the simultaneous and independent training of any number of f_M networks with different structures and loss supervision optimizations, using the same dataset. **Bottom**: The flexibility during the inference stage allows the combination of any number of TINet, regardless of their optimization process.

each f_M is updated based on its loss function, allowing the frozen encoders to be shared in a single process, improving efficiency by reducing redundant data passes through the encoders.

In testing, the method supports varying numbers of TINets with different structures and optimizations. After passing through the visual encoder, an image can be processed by multiple TINets to generate multiple pseudo-words (S_*), whose average produces the final query embedding for retrieval. More TINets improve performance but reduce efficiency, thus a balance between accuracy and speed can be achieved depending on application needs.

IV. DATASET

A. ITCPR Dataset

In contrast to existing CIR datasets [44], [45], where reference and target images only need to be loosely related, the CPR datasets subject to the constraint that both of them depict the same person. Therefore, when constructing the ITCPR dataset, we ask the selected images to have the same identity, but wear different clothes or be in different scenes. In our implementation, publicly available clothes-changing datasets such as Celeb-reid [9], PRCC [11], and LAST [10] are utilized as our image sources.

1) *Dataset Annotation Process*: The annotation process, as shown in Fig. 4, primarily consists of three steps. The first step involves selecting identities from the image data sources that have multiple images with different outfits, ensuring a diverse selection for subsequent steps. In the second step, a pair of images associated with each chosen identity is selected and denoted as I_q and I_t . It is worth noting that, ideally, these two images should depict partially matching outfits, allowing I_q to provide additional clothing-related information beyond facial features and body posture. This additional clothing information is not mentioned in the corresponding annotation T_q , ensuring

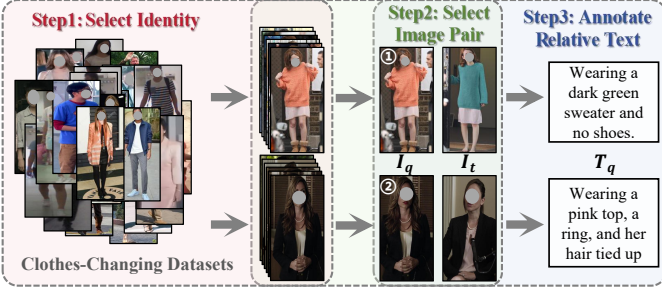


Fig. 4. The annotation process of the ITCPR dataset. The annotation process can be summarized in three steps: the first step is selecting identities from the clothes-changing datasets, the second step is choosing pairs of reference and target images for each identity, and the third step is manually annotating the relative captions.

that CPR methods can only correctly identify I_t by utilizing both I_q and T_q . Once the image pair is selected, the process moves to the third step, where manual annotations are created to specifically capture the differences between I_q and I_t . For instance, as shown in case 1 of Fig. 4, if the skirt is the same in both the target image and the reference image, it does not need to be described; the annotation focuses only on differences in the top and shoes. After manually annotating T_q , a complete triplet annotation process is finalized. Repeating this process, a batch of triplets (I_q, T_q, I_t) can be generated for testing CPR methods. 0

2) *Re-Annotation of the ITCPR Dataset*: The gallery contains a large number of noisy images, which may introduce false negatives. For example, for certain queries, some images may be potential ground truth but remain unlabeled. Including such cases would reduce the reliability of the evaluation metrics. To address this issue, all images in the gallery are screened, and any false negative images identified in the dataset are re-annotated. The re-annotation process is illustrated in Fig. 5. After completing the dataset annotation and adding noise images to the gallery, we use a well-trained visual encoder to search for the most similar images for each target image, followed by manual inspection and verification. Through this approach, we effectively eliminate false negatives in the ITCPR dataset. Fig. 6 shows some examples from the ITCPR dataset.

3) *Statistics of the ITCPR Dataset*: In summary, ITCPR comprises a total of 2,225 annotated triplets. These triplets encompass 2,202 unique combinations (I_q, T_q) as queries. ITCPR contains 1,151 images and 512 identities from CelebreID [9], 146 images and 146 identities from PRCC [11], and 905 images and 541 identities from LAST [10]. In the target gallery, there are a total of 20,510 images of persons from the three datasets, with 2,225 corresponding ground truths for the queries. The textual annotations have an average sentence length of 9.54 words, with a total of 461 unique words. The longest sentence contains 32 words, while the shortest sentence only contains 3 words. These annotations are exclusively designated for testing in the ZS-CPR task, which expects to achieve substantial performance without utilizing any data from the three datasets mentioned above.

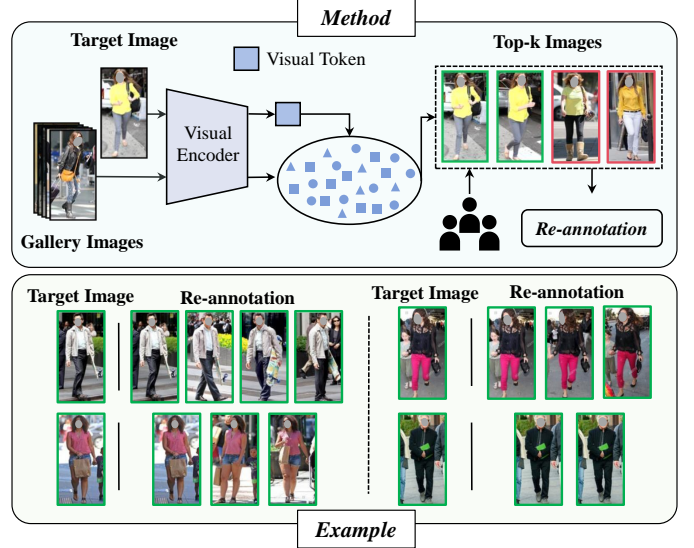


Fig. 5. False negative elimination scheme in ITCPR. **Top**: The method of eliminating false negative images and adding annotations in the dataset. **Bottom**: Examples of false negative images re-annotated in ITCPR.

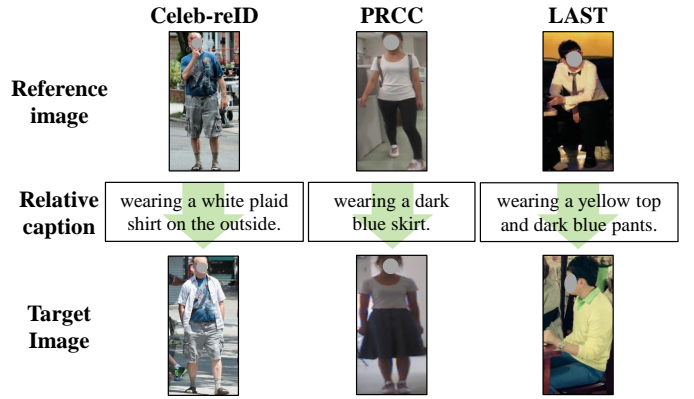


Fig. 6. Examples of queries and ground truths in our ITCPR dataset.

B. Other Datasets

Image-text Datasets. Notably, there are three publicly accessible datasets: CUHK-PEDES [4], ICFG-PEDES [7], and RSTPReid [8]. Our primary concern focuses on the CUHK-PEDES dataset, while the other two datasets are mainly employed for ablation experiments. In the subsequent experiments (Table IV), we abbreviate datasets as follows, CUHK-PEDES is denoted as C , ICFG-PEDES as I , and RSTPReid as R .

Image Datasets. In the Word4Per method, when exclusively utilizing \mathcal{L}_{Vis} for textual inversion optimization, the training uses the datasets containing only images. It's essential to mention that datasets containing images of persons are abundant and widely available in IPR, including Market1501 [51], MSMT17 [52], CUHK02 [53], CUHK03-NP [54], CUHK-SYSU [55], GRID [56], VIPeR [57], QMUL i-LIDS [58], and PRID [59]. In subsequent ablation experiments, we combine above datasets with the images from image-text datasets mentioned before to yield a total of 1,057,361 images, is collectively called the IPR dataset.

TABLE I

ZERO-SHOT RETRIEVAL RESULTS OF RELEVANT METHODS ON THE ITCPR DATASET. \mathcal{L}_{Vis} AND \mathcal{L}_{Text} REPRESENT THE LOSSES USED FOR SUPERVISED OPTIMIZATION OF THE TINET. THE \dagger SYMBOL INDICATES THAT THE TRAINING OF THE METHODS WAS PERFORMED ON THE ORIGINAL PRE-TRAINED PARAMETERS OF CLIP, WHICH MAY POSE CHALLENGES FOR DOMAIN GENERALIZATION AND RESULT IN CERTAIN PERFORMANCE DEGRADATION.

No.	Backbone	Dual Encoder	Method	Rank-1	Rank-5	Rank-10	mAP
1	ViT-B/16	CLIP [12]	Image-only	7.357	16.803	22.934	12.524
2			Text-only	4.632	10.309	14.759	8.116
3			Image+Text	16.757	32.516	40.372	24.674
4		Fine-tuned	Image-only	5.041	10.763	13.442	8.086
5			Text-only	26.385	46.458	56.267	36.132
6			Image+Text	29.837	50.136	59.037	39.632
7			Text+ <i>Model C</i> [50]	32.743	55.904	64.487	43.484
8			Ours (\mathcal{L}_{Vis})	38.919	59.310	67.075	48.538
9			Ours (\mathcal{L}_{Text})	40.054	61.262	68.584	49.903
10			Ours ($\mathcal{L}_{Vis} + \mathcal{L}_{Text}$)	40.872	61.989	68.847	50.521
11	ViT-L/14	CLIP [12]	Image-only	8.265	18.483	24.523	13.795
12			Text-only	3.270	9.219	14.532	6.929
13			Image+Text	18.165	35.195	43.324	26.652
14			Pic2Word [47]	21.208	37.148	44.505	29.108
15			SEARLE-XL [48]	22.252	37.693	45.232	30.543
16		Fine-tuned	Image-only	5.268	10.763	13.987	8.345
17			Text-only	28.974	50.817	59.900	39.333
18			Image+Text	32.016	52.634	60.990	41.831
19			Text+ <i>Model C</i> [50]	35.377	53.588	61.172	44.084
20			Pic2Word [47] \dagger	32.652	55.041	62.807	43.086
21			SEARLE-XL [48] \dagger	33.379	54.496	62.943	43.333
22			Ours (\mathcal{L}_{Vis})	43.960	64.714	72.480	53.554
23			Ours (\mathcal{L}_{Text})	45.549	66.803	74.796	55.260
24			Ours ($\mathcal{L}_{Vis} + \mathcal{L}_{Text}$)	45.913	66.848	75.114	55.630

V. EXPERIMENTS

A. Experiments Setup

Datasets. The Word4Per method employs image-text datasets for both fine-tuning and TINet training (where \mathcal{L}_{Vis} only uses images). In this part, the image-text dataset CUHK-PEDES [4] is used as the default training dataset.

Implementation Details. The experiments are conducted on a single A100 GPU. The input image size is adjusted to 384×128 , with each image patch measuring 16×16 . The maximum length for text tokens is set to 77. Training is performed by the Adam [60] optimizer for 60 epochs, with a batch size of 128. Cosine learning rate decay is applied. Initially, 5 warm-up epochs are conducted, gradually increasing the learning rate from 1/10 of the initial learning rate to the initial value. The temperature parameter τ in the losses is set to 0.02.

During the fine-tuning, the image and text encoders are initialized with pretrained CLIP [12] parameters. The initial learning rate is set to 10^{-5} . For modules with random initialization, the initial learning rate is set to 5×10^{-5} . In the training of the TINet, the parameters of the visual and text encoder inherit the fine-tuned parameters and remain frozen. A fully connected neural network is used to construct a lightweight TINet. When the visual encoder is ViT-B/16, the input and output dimensions are set to 512. When it is ViT-L/14, the input and output dimensions are 768, while the hidden layer dimension remains at 512. The parameters are randomly initialized. The initial learning rate is set to 10^{-4} . The CUHK-PEDES dataset is used for training. If the visual encoder is ViT-B/16, training a single TINet takes

approximately 2 hours. If the visual encoder is ViT-L/14, training takes about 5 hours. When leveraging the model's flexibility to train multiple TINets simultaneously, sharing the dual encoder's output increases the training time by only 15% per additional TINet.

Evaluation Metrics. For ZS-CPR testing metrics, performance is evaluated by the Rank-k measure. This measure is employed to assess the probability of finding at least one matching person image among the top-k similar candidates for given query. Common values for k are 1, 5, and 10. Higher Rank-k scores indicate that the system effectively retrieves targets. In addition, we also employ the mean average precision (mAP) for evaluation. mAP is computed by calculating the average precision of retrieved relevant images and averaging the results across all queries, considering the performance of model on various queries. Higher Rank-k and mAP values signify superior method performance.

B. Quantitative Results

Word4Per is compared with several baseline methods [12] that support zero-shot retrieval, as well as Pic2Word [47] and SEARLE [48], methods with notable performance in the ZS-CIR task. The baseline methods include several testing modes: 1) Image-only: using only the reference image via a pre-trained visual encoder to retrieve person. 2) Text-only: using only relative caption via a pre-trained text encoder. 3) Image + Text: Target person retrieval by averaging features obtained from the above two methods. 4) Text+*Model C*: Target person retrieval by averaging results obtained from the Text-only and

TABLE II
PERFORMANCE OF VARIOUS PRE-TRAINED MODELS ON CUHK-PEDES [4]. FINE-TUNE DENOTES THE CLIP MODEL FINE-TUNED ACCORDING TO THE SETTINGS IN THIS PAPER.

No.	Backbone	Method	Rank-1	Rank-5	mAP
1	ViT-B/16	CLIP	12.606	27.112	11.145
2		Fine-tuned	73.847	89.571	68.086
3	ViT-L/14	CLIP	10.185	23.262	9.192
4		Fine-tuned	75.991	90.578	68.337

Model C (Simple-CCReID [50] is trained on the LTCC [61] dataset to prevent data leakage). 5) CIR methods [47], [48]: using the parameters of the TINet trained with the original CIR method. Our method is trained and tested on both ViT-B/16 and ViT-L/14 visual encoders. Because Pic2Word and SEARLE are only provided for the ViT-L/14 scheme, thus we conduct the comparison with them only under the ViT-L/14 experimental setting.

Table I shows the test results of comparative methods on the ITCPR dataset, demonstrating that our method significantly outperforms all baseline models and ZS-CIR methods. The experimental results of No. 1-6, No. 11-13, and No. 16-18 reveal that utilizing both text and image information, regardless of whether the encoder is trained with CLIP [12] or fine-tuning, leads to optimal performance. These results also show the rational construction of our ITCPR dataset, leveraging both textual and visual cues from the query, the target person can be effectively identified. Comparing with the results of experiments No. 1-3 with No. 4-6, and No. 11-13 with No. 16-18, it is evident that fine-tuning the dual encoders is effective and necessary. Specifically, the results of No. 7 and No. 19 demonstrate that our method significantly outperforms the dual-model approach incorporating clothes-changing models with a lower computational cost. Moreover, the results of No. 8-10 and No. 22-24 indicate that supervising the TINet with \mathcal{L}_{Text} is more effective, and a combination of both supervisions achieves the best performance.

C. Ablation Studies

To further show the effectiveness of the proposed Word4Per method for the ZS-CPR problem, we conduct extensive ablation studies. Due to limited training resources, the majority of ablation experiments are conducted on the fine-tuned dual encoders with a visual encoder of ViT-B/16. Note that experiments without specifying the dual encoders are based on this setup, and the parameters of the encoders are obtained from the fine-tuning network and remain frozen.

Fine-tuning Results. In the fine-tuning process of Word4Per, the objective is to make the model capable of performing TPR task effectively. In line with this, we also evaluate the performance of the fine-tuned models on the CUHK-PEDES test set, and the results are shown in Table II. It can be observed that fine-tuning the parameters of CLIP [12] is essential.

Ablation Study for TINet architecture. Fig. 7 illustrates the performance of TINets with different depths and hidden layer widths under various supervisions. For \mathcal{L}_{Vis} supervision,

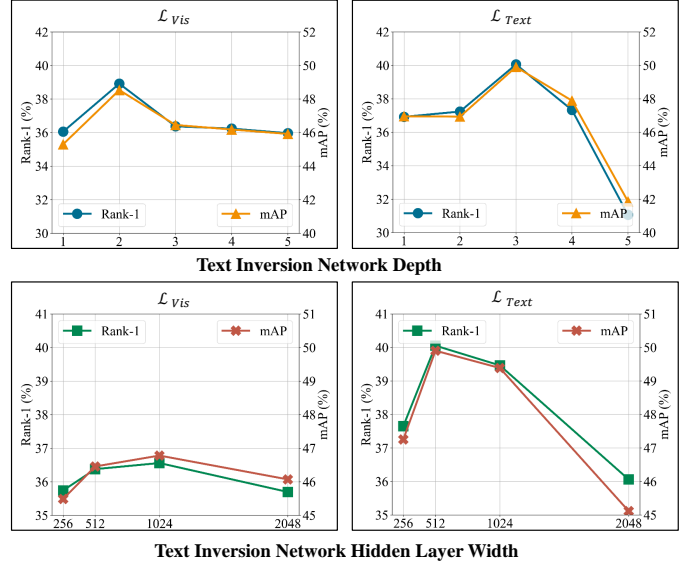


Fig. 7. Method performance using TINet with different depths and hidden layer widths under various supervisions. **Top:** Performance using TINet with different depths, with a hidden layer width of 512. **Bottom:** Performance using TINet with different hidden layer widths, all with a depth of three layers.

a two-layer fully connected neural network emerges as the optimal structure. On the other hand, for \mathcal{L}_{Text} supervision, a three-layer fully connected neural network is found to be most suitable. The hidden layer width exhibits sensitivity primarily to \mathcal{L}_{Text} supervision, with the optimal width being 512 units. In the quest for a harmonious balance between efficiency and precision, we opt to maintain a consistent hidden layer width of 512 across different configurations.

Word4Per with Smaller Data Volumes. We conduct training of the TINet by extracting original data at different proportions to observe if utilizing more data will yield better results. As shown in Table III, the experimental results show that even when using a randomly initialized TINet, it does not result in significant performance loss (No. 1 and No. 2). With a small amount of data available for training (No. 3 and No. 9), Word4Per performance still surpasses all previous methods. Furthermore, the results of experiments No. 9-14 lead to the following conclusions: when optimizing the TINet under \mathcal{L}_{Text} supervision on the same dataset, training with more image-text pairs can result in superior performance. For \mathcal{L}_{Vis} supervised optimization (No. 3-7), this trend is similar to \mathcal{L}_{Text} , while No. 8 exhibits marginally superior performance compared to No. 7 due to the impact of low-quality images and noise in the dataset.

Flexibility in Testing. Section III-D thoroughly discusses the flexibility of Word4Per in both training and testing. Leveraging this flexibility, multiple high-performance TINets can be utilized simultaneously during testing for fusion retrieval, thereby achieving the best performance within the current framework. The corresponding results and efficiencies for different methods are shown in Table IV, where the “&” symbol in the “Method” column indicates fusion testing using TINets obtained by the methods corresponding to the rows on either side of the symbol. The results demonstrate that,

TABLE III
IMPACT OF EXTRACTING DATA AT DIFFERENT PROPORTIONS FROM THE SAME DATASET FOR TRAINING. “RANDOM” INDICATES THE USAGE OF RANDOMLY INITIALIZED TINET.

No.	Method	Rank-1	Rank-5	Rank-10	mAP	Dataset	No.	Method	Rank-1	Rank-5	Rank-10	mAP
1	Random	25.749	45.822	55.767	35.581	-	2	Text-only	26.385	46.458	56.267	36.132
3	\mathcal{L}_{Vis}	32.334	50.727	58.629	41.261	10%	9	\mathcal{L}_{Text}	32.970	51.680	59.310	41.727
4		33.106	54.269	62.807	43.192	20%	10		34.242	55.040	63.259	43.744
5		34.514	54.541	64.850	44.760	30%	11		35.195	55.632	64.124	44.650
6		36.376	57.902	66.213	46.679	50%	12		37.125	57.026	65.468	46.951
7		<u>38.374</u>	<u>59.855</u>	<u>67.757</u>	<u>48.502</u>	75%	13		<u>38.583</u>	<u>59.819</u>	<u>67.813</u>	<u>48.631</u>
8		38.919	<u>59.310</u>	<u>67.075</u>	48.538	100%	14		40.054	61.262	68.584	49.903

TABLE IV
PERFORMANCE UNDER DIFFERENT STRATEGIES. IPR REPRESENTS THE IMAGE DATASET AS DESCRIBED IN SECTION IV-B, AND $IPR^{10\%+}$ INVOLVES SELECTING THE HIGHEST 10% RESOLUTION IMAGES TO FORM A NEW DATASET. THE TIME IN THE TABLE REPRESENTS THE DURATION REQUIRED FOR THE RESPECTIVE METHOD TO COMPLETE ALL RETRIEVAL TASKS ON THE ENTIRE ITCPR DATASET.

No.	Backbone	Dataset	Method	Time (s)	Rank-1	Rank-5	Rank-10	mAP
1	ViT-B/16	C	Image-only	28.377	5.041	10.763	13.442	8.086
2		C	Text-only	27.212	26.385	46.458	56.267	36.132
3		C	\mathcal{L}_{Text}	30.656	40.054	61.262	68.584	49.903
4		$C + I + R$	\mathcal{L}_{Vis}	30.454	41.826	62.307	69.391	51.353
5		$IPR^{10\%+}$	\mathcal{L}_{Vis}	30.453	41.508	62.080	69.028	50.825
6		-	No.3&4	31.020	43.415	63.442	70.663	52.740
7		-	No.3&5	31.081	<u>43.415</u>	<u>63.488</u>	<u>70.754</u>	52.622
8		-	No.4&5	30.997	42.461	63.124	70.481	52.073
9		-	No.3&4&5	31.574	43.551	63.760	71.026	53.041
10	ViT-L/14	C	Image-only	61.739	5.268	10.763	13.987	8.345
11		C	Text-only	57.874	28.974	50.817	59.900	39.333
12		C	\mathcal{L}_{Text}	65.130	45.549	66.803	74.796	55.260
13		$C + I + R$	\mathcal{L}_{Vis}	64.986	45.595	65.168	72.616	54.755
14		$IPR^{10\%+}$	\mathcal{L}_{Vis}	64.979	45.549	66.167	73.025	54.906
15		-	No.12&13	66.063	47.184	68.256	<u>75.023</u>	56.790
16		-	No.12&14	66.069	47.048	<u>68.483</u>	74.796	56.636
17		-	No.13&14	65.913	46.458	66.803	74.069	55.688
18		-	No.12&13&14	66.475	47.502	68.392	75.103	56.944

although \mathcal{L}_{Vis} supervision is less effective than \mathcal{L}_{Text} with the same data volume, it can still leverage large amounts of person image data for extended training. Consequently, this yields experimental results No. 4-5 and No. 13-14, representing the best performance achievable with a single TINet. A significant performance improvement is observed when two textual inversion networks are fused (No. 6-8 and No. 15-17). Among them, the TINets optimized by the same supervision show the smallest fusion improvement (No. 8 and No. 17), even though their individual network performance is outstanding. On the other hand, fusing two TINets optimized with different supervision methods yields the best results (No. 6-7 and No. 15-16). When using three textual inversion networks, performance is further enhanced, though to a lesser extent (No. 9 and No. 18). It can thus be inferred that fusing more well-trained TINets leads to better performance, albeit with diminishing returns, and will also reduce retrieval efficiency.

Ablation Study for Pseudo-word (S_*). Employing various templates for S_* and altering token length results in distinct performance, as shown in Table V. Comparative analysis of results No. 1-5 reveals that, compared to directly appending relative captions to S_* , utilizing intuitively coherent templates can enhance performance. Furthermore, experimental results No. 5-8 indicate that when the token length of S_* is fewer than four, performance remains relatively stable but declines with longer token lengths due to the detrimental impact of

TABLE V
TEMPLATE AND TOKEN LENGTH OF S_* IMPACT ON PERFORMANCE. SUPERVISED OPTIMIZATION IS CONDUCTED WITH \mathcal{L}_{Text} . VARYING TOKEN LENGTHS ARE ACHIEVED BY MODIFYING THE OUTPUT DIMENSIONS OF THE TINET.

No.	Template	Length	Rank-1	Rank-5	mAP
1	$[S_*] \{Caption\}$	1	39.055	60.263	48.995
2	$a \text{ photo of } [S_*] \{Caption\}$	1	39.373	60.173	49.509
3	$a \text{ photo of } [S_*] \text{ is } \{Caption\}$	1	39.146	61.124	49.460
4	$[S_*] \text{ is } \{Caption\}$	1	39.555	60.490	49.266
5	$a [S_*] \text{ is } \{Caption\}$	1	<u>40.054</u>	61.262	49.903
6	$a [S_*] \text{ is } \{Caption\}$	2	40.100	60.990	49.708
7		4	39.691	61.126	49.734
8		8	38.193	59.083	47.929

excessive inversion elements on linguistic stability. Therefore, considering all the factors above, the configuration of experiment No. 4 is chosen as the final setup.

D. Qualitative Results

Visualization of ZS-CPR Models. The visualization of the results obtained by ZS-CPR models are compared. Fig. 8 shows two typical cases. In case 1, it is evident that, regardless of the parameters scale, using image-only retrieval yields the poorest results. Because it trends to obtain the images possessing visually similar pixel distributions, and the dataset contains numerous instances of clothes-changing, resulting in subpar

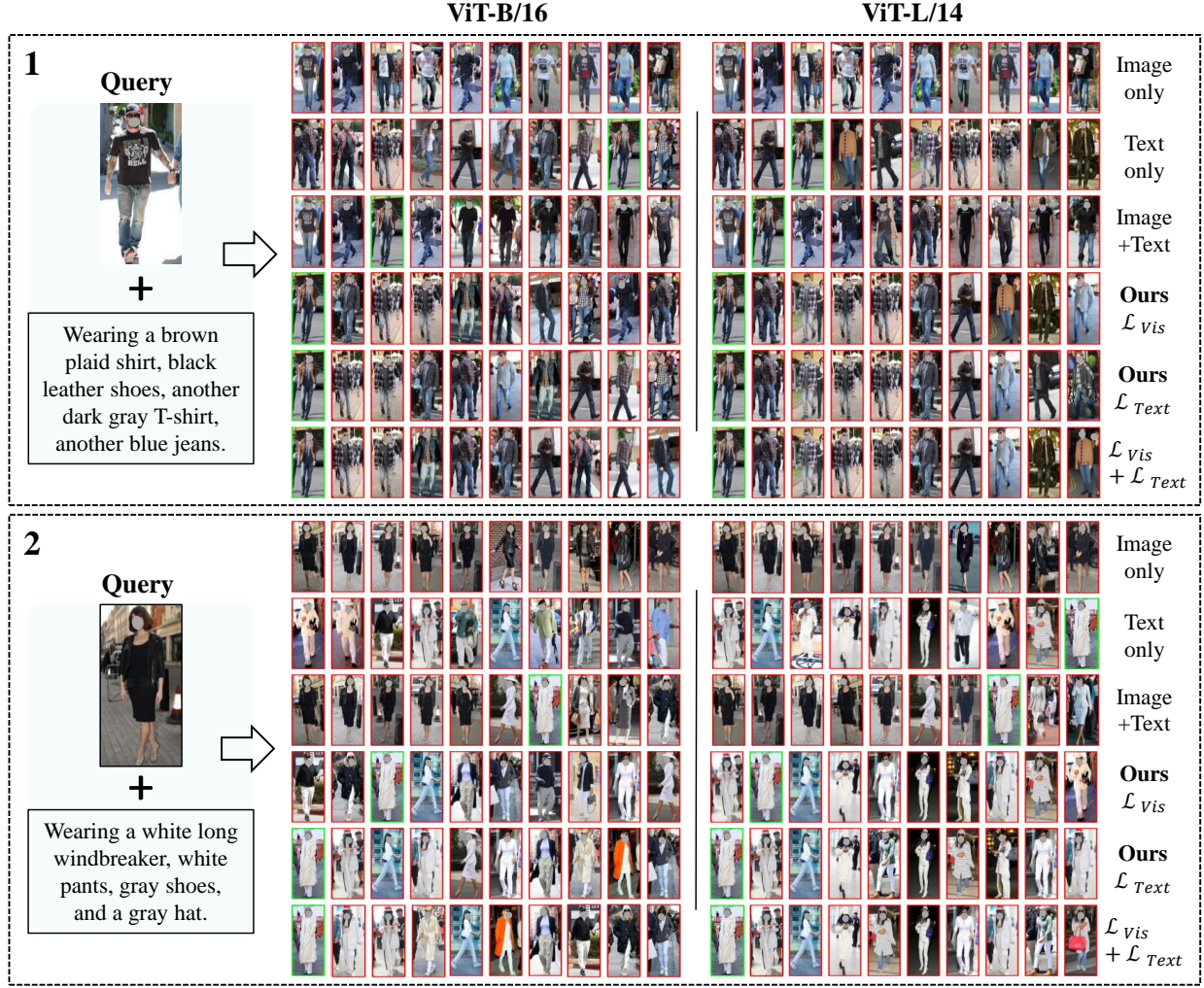


Fig. 8. Top-10 retrieval results on the ITCPR dataset for relevant methods. The figure presents retrieval results for two query examples under different methods, all employing fine-tuned encoders.

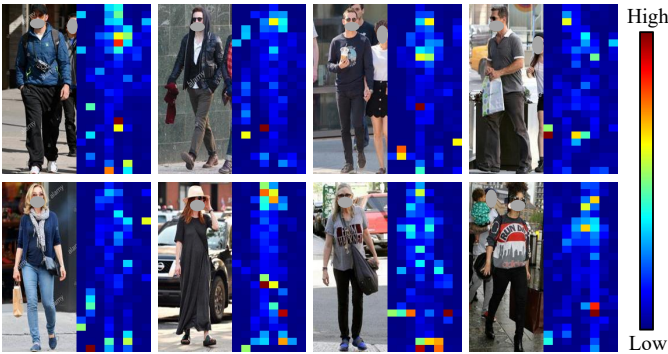


Fig. 9. Visualization of the global token average attention map in the last layer of the visual encoder in Word4Per with ViT-B/16 configuration.

performance. Text-only retrieval also falls short of expectations since most annotations in the dataset describe attire briefly, and there are numerous images with similar clothing. The combined use of both modalities in retrieval often yields the desired target images among the top results. When using the Word4Per method, the TINet, supervised with either \mathcal{L}_{Text} or

\mathcal{L}_{Vis} , consistently succeeds in finding the target image. case 2 exhibits a similar pattern to case 1. However, in scenarios where the training dataset is unfiltered and remains consistent, the ambiguity of vision negatively effects the effectiveness of the model. In contrast, the textual information is more stable than visual one, thus TINet optimized with \mathcal{L}_{Text} tend to achieve the better retrieval results. Combining both directly provides the most stable retrieval outcomes.

Effectiveness of TINet. To explore what information the pseudo-word tokens generated by TINet capture from person images, we visualize the global token average attention map of the last layer of the visual encoder in Word4Per, as shown in Fig. 9. This visualization represents the information contained in the input to TINet. From the figure, it is evident that the global features primarily focus on a person's attire and appearance while also on part of the background. The supervision used in TINet determines which information is emphasized in the mapping. When supervised with \mathcal{L}_{Vis} , the features learned by TINet are aligned with the complete information of the image, including unrelated background details. On the other hand, when supervised with \mathcal{L}_{Text} , TINet

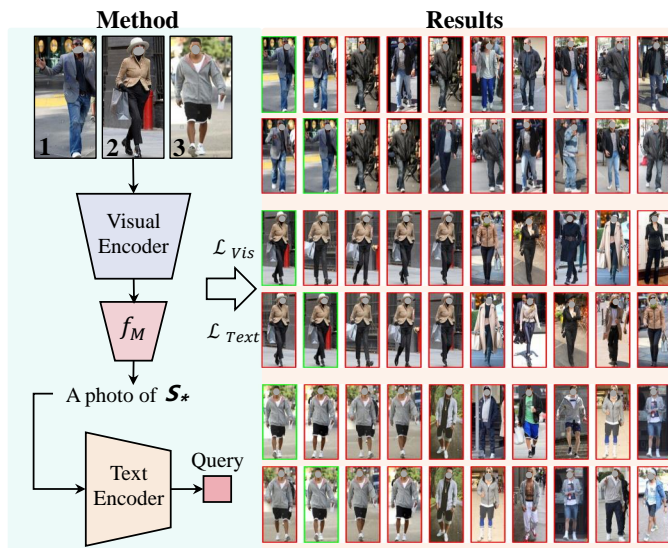


Fig. 10. Method and results of pseudo-word token retrieval for the original Image. On the left is an illustration of the retrieval method, and on the right are the retrieval results for three examples.

focuses more on the individual, since the text mainly describes the person themselves. To verify this observation, we conduct another comparative experiment, as shown in Fig. 10. In this experiment, pseudo-word tokens from all reference images are used to retrieve images from a mixed dataset containing both reference and gallery images. When using TINet supervised with \mathcal{L}_{Vis} , the model consistently finds the original image among the most similar retrieval results, even when the appearance of the person is highly consistent, as it utilizes differences in the background. However, when supervised with \mathcal{L}_{Text} , the original image cannot be found among the most similar retrieval results. This is mainly because the semantic annotations of person images typically do not focus on the background but rather emphasize characteristics related to the individual. This is also a key reason for its strong performance in the ZS-CPR task.

E. Application Effects

In terms of the type of application, the main advantage of our method is that it can meet different person search needs, relying only on image information (visual encoder), text information (dual encoder), or a fusion of both (Word4Per) to achieve person retrieval.

In terms of efficiency, our evaluations are conducted on an Intel(R) Xeon(R) Platinum 8358P CPU @ 2.60GHz with a single A100 GPU. Take Word4Per with the ViT-B/16 configuration as an example, in a practical retrieval scenario, for example, performing a search for 1,000 queries in a database containing 20,000 images, it will take 26.26 seconds for 1000 image-only queries (merely 26ms for one image query), 25.23 seconds for text-only queries (25ms for one query), and 26.49 seconds for composed queries (26ms for one composed query). In fact, the majority of the time is spent on feature extraction, while similarity computation and target ranking are only millisecond-level consumption. Therefore, if

TABLE VI
EXPERIMENTAL RESULTS OF REPLACING PSEUDO-WORD TOKENS WITH EXISTING WORDS. “1ST SIM” INDICATES USING WORDS WITH THE HIGHEST SIMILARITY TO REPLACE PSEUDO-WORD TOKENS FOR TARGET RETRIEVAL.

No.	Backbone	Method	Rank-1	Rank-5	mAP
1	ViT-B/16	Text-only	26.385	46.458	36.132
2		1st Sim	27.884	49.001	37.955
3		\mathcal{L}_{Text}	40.054	61.262	49.903
4	ViT-L/14	Text-only	28.974	50.817	39.333
5		1st Sim	32.016	53.769	42.242
6		\mathcal{L}_{Text}	45.549	66.803	55.260

the image features in the image database are pre-extracted, one image-only query will only take 1.24 ms, 0.23 ms for one text-only query, and 1.48 ms for one composed query. This can meet practical application needs. For users demanding higher performance, the ViT-L/14 configuration can be used, although this reduces retrieval efficiency by 46% compared to the standard model.

VI. DISCUSSION

Based on above results, it is evident that a well-trained TINet can effectively transform the image into a single pseudo-word token and can concisely and efficiently combine the relative caption to improve CPR performance. However, what semantic information is contained in these pseudo-words and whether they can be replaced with real words from the vocabulary? To address these questions, within the entire vocabulary we find the words that are most similar to the pseudo-words, so as to infer the relevant semantic information hidden in the pseudo-words (Fig. 11(a)).

Several results with randomly chosen images are shown in Fig. 11(b). It becomes apparent that words similar to the pseudo-words can effectively describe the original image, containing various details about the person. These details include gender information (e.g., *man*, *woman*, *girl*), clothing details (e.g., *boots*, *sweater*, *suit*), color descriptions (e.g., *blue*, *purple*, *indigo*), and items carried by the person (e.g., *newspaper*, *sunglasses*, *handbags*). Furthermore, the obtained words contain additional aspects, such as the state of the persons, style, spatial location, attire materials, etc. It is worth noting that, some vocabulary may not directly describe the image, but certain parts of these words (bolded in the Fig. 11(b)) can be prompted to the corresponding image. This phenomenon may be owned to the usage of Byte Pair Encoding (BPE) [62] in the text encoding. By extending observation to top-50 even top-100 words, we can unearth more meaningful semantic information. This suggests that pseudo-word tokens obtained by the TINet are actually a combination of multiple meaningful semantic information and contain a variety of information.

If pseudo-word tokens are replaced with the most similar words from the vocabulary, will the results still be stable? To investigate this, relevant experiments are conducted, and the results are shown in Table VI. The results show although adding a valid word can bring some performance improvement, it is far less obvious than the use of pseudo-word

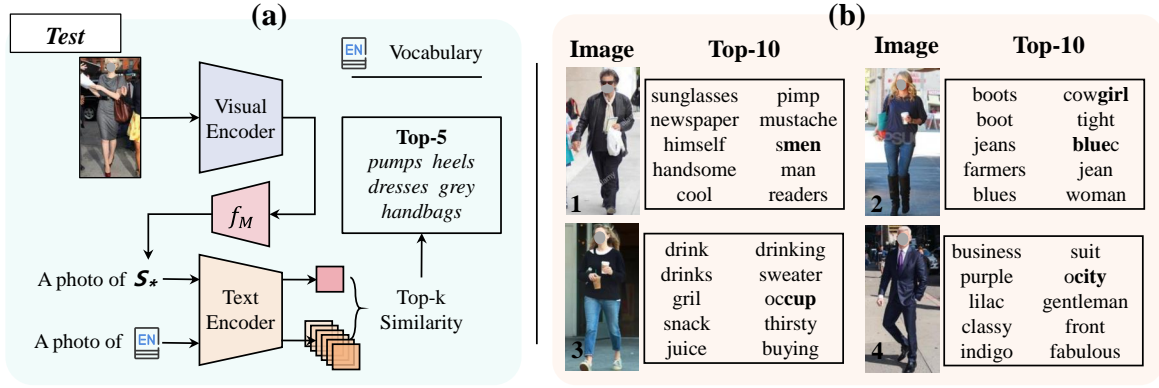


Fig. 11. (a) Semantic information exploration of pseudo-word tokens. Experiments are conducted using the \mathcal{L}_{Text} supervised optimized TINET (ViT-B/16). (b) Top-10 vocabulary words most similar to pseudo-words in some images.

tokens. The results are also quite comprehensible, that is, it is challenging to summarize a person image just using one existing word, whereas one pseudo-word token can accomplish this.

VII. CONCLUSION

In this paper, we address limitations in handling queries that involve both image and text information for person retrieval, through the introduction of CPR task. To overcome data annotation challenges in CPR, we put forward the ZS-CPR problem, eliminating reliance on expensive triplet annotations. Furthermore, a two-stage framework called Word4Per is developed to train ZS-CPR model, achieving very promising performance on our proposed ITCPR dataset without the need for CPR datasets. Comprehensive ablation studies are also conducted on Word4Per, and a slice of valuable insights are obtained. However, The proposed CPR task is still in its infancy, and there are many directions that can be optimized.

ACKNOWLEDGMENT

The work is supported by The Key R&D Program of Yunnan Province (202102AE09001902-2), and the BUPT Innovation and Entrepreneurship Support Program (2024-YC-T030).

REFERENCES

- [1] Y. Zhang, B. He, L. Sun, and Q. Li, "Progressive multi-stage feature mix for person re-identification," in *ICASSP 2021 - 2021 IEEE International Conference on Acoustics, Speech and Signal Processing (ICASSP)*, 2021.
- [2] D. Jiang and M. Ye, "Cross-modal implicit relation reasoning and aligning for text-to-image person retrieval," in *Proceedings of the IEEE/CVF Conference on Computer Vision and Pattern Recognition*, pp. 2787–2797, 2023.
- [3] H. Luo, Y. Gu, X. Liao, S. Lai, and W. Jiang, "Bag of tricks and a strong baseline for deep person re-identification," in *Proceedings of the IEEE/CVF conference on computer vision and pattern recognition workshops*, pp. 0–0, 2019.
- [4] S. Li, T. Xiao, H. Li, B. Zhou, D. Yue, and X. Wang, "Person search with natural language description," in *Proceedings of the IEEE conference on computer vision and pattern recognition*, pp. 1970–1979, 2017.
- [5] N. Vo, L. Jiang, C. Sun, K. Murphy, L.-J. Li, L. Fei-Fei, and J. Hays, "Composing text and image for image retrieval-an empirical odyssey," in *Proceedings of the IEEE/CVF conference on computer vision and pattern recognition*, pp. 6439–6448, 2019.
- [6] M. Hosseinzadeh and Y. Wang, "Composed query image retrieval using locally bounded features," in *2020 IEEE/CVF Conference on Computer Vision and Pattern Recognition (CVPR)*, 2020.
- [7] Z. Ding, C. Ding, Z. Shao, and D. Tao, "Semantically self-aligned network for text-to-image part-aware person re-identification," *arXiv preprint arXiv:2107.12666*, 2021.
- [8] A. Zhu, Z. Wang, Y. Li, X. Wan, J. Jin, T. Wang, F. Hu, and G. Hua, "Dssl: Deep surroundings-person separation learning for text-based person retrieval," in *Proceedings of the 29th ACM International Conference on Multimedia*, pp. 209–217, 2021.
- [9] Y. Huang, Q. Wu, J. Xu, and Y. Zhong, "Celebrities-reid: A benchmark for clothes variation in long-term person re-identification," in *2019 International Joint Conference on Neural Networks (IJCNN)*, pp. 1–8, IEEE, 2019.
- [10] X. Shu, X. Wang, X. Zang, S. Zhang, Y. Chen, G. Li, and Q. Tian, "Large-scale spatio-temporal person re-identification: Algorithms and benchmark," *IEEE Transactions on Circuits and Systems for Video Technology*, vol. 32, no. 7, pp. 4390–4403, 2021.
- [11] Q. Yang, A. Wu, and W.-S. Zheng, "Person re-identification by contour sketch under moderate clothing change," *IEEE transactions on pattern analysis and machine intelligence*, vol. 43, no. 6, pp. 2029–2046, 2019.
- [12] A. Radford, J. W. Kim, C. Hallacy, A. Ramesh, G. Goh, S. Agarwal, G. Sastry, A. Askell, P. Mishkin, J. Clark, *et al.*, "Learning transferable visual models from natural language supervision," in *International conference on machine learning*, pp. 8748–8763, PMLR, 2021.
- [13] Y. Sun, L. Zheng, Y. Yang, Q. Tian, and S. Wang, *Beyond Part Models: Person Retrieval with Refined Part Pooling (and a Strong Convolutional Baseline)*, p. 501–518. 2018.
- [14] J. Qian, W. Jiang, H. Luo, and H. Yu, "Stripe-based and attribute-aware network: a two-branch deep model for vehicle re-identification," *Measurement Science and Technology*, p. 095401, 2020.
- [15] A. Hermans, L. Beyer, and B. Leibe, "In defense of the triplet loss for person re-identification," *arXiv: Computer Vision and Pattern Recognition*, 2017.
- [16] K. Zhou, Y. Yang, A. Cavallaro, and T. Xiang, "Omni-scale feature learning for person re-identification," in *2019 IEEE/CVF International Conference on Computer Vision (ICCV)*, 2019.
- [17] R. Quan, X. Dong, Y. Wu, L. Zhu, and Y. Yang, "Auto-reid: Searching for a part-aware convnet for person re-identification," in *2019 IEEE/CVF International Conference on Computer Vision (ICCV)*, 2019.
- [18] H. Li, G. Wu, and W.-S. Zheng, "Combined depth space based architecture search for person re-identification," in *2021 IEEE/CVF Conference on Computer Vision and Pattern Recognition (CVPR)*, 2021.
- [19] X. Ning, K. Gong, W. Li, L. Zhang, X. Bai, and S. Tian, "Feature refinement and filter network for person re-identification," *IEEE Transactions on Circuits and Systems for Video Technology*, vol. 31, no. 9, pp. 3391–3402, 2020.
- [20] P. Wang, Z. Zhao, F. Su, and H. Meng, "Ltreid: Factorizable feature generation with independent components for long-tailed person re-identification," *IEEE Transactions on Multimedia*, 2022.
- [21] Z. Zhang, C. Lan, W. Zeng, X. Jin, and Z. Chen, "Relation-aware global attention for person re-identification," *arXiv: Computer Vision and Pattern Recognition*, 2019.
- [22] T. Chen, S. Ding, J. Xie, Y. Yuan, W. Chen, Y. Yang, Z. Ren, and Z. Wang, "Abd-net: Attentive but diverse person re-identification," in *2019 IEEE/CVF International Conference on Computer Vision (ICCV)*, 2019.

- [23] Y. Li, J. He, T. Zhang, X. Liu, Y. Zhang, and F. Wu, "Diverse part discovery: Occluded person re-identification with part-aware transformer," in *Proceedings of the IEEE/CVF Conference on Computer Vision and Pattern Recognition*, pp. 2898–2907, 2021.
- [24] M. Jia, X. Cheng, S. Lu, and J. Zhang, "Learning disentangled representation implicitly via transformer for occluded person re-identification," *IEEE Transactions on Multimedia*, vol. 25, pp. 1294–1305, 2022.
- [25] S. He, H. Luo, P. Wang, F. Wang, H. Li, and W. Jiang, "Transreid: Transformer-based object re-identification," in *2021 IEEE/CVF International Conference on Computer Vision (ICCV)*, 2021.
- [26] K. He, X. Zhang, S. Ren, and J. Sun, "Deep residual learning for image recognition," in *Proceedings of the IEEE conference on computer vision and pattern recognition*, pp. 770–778, 2016.
- [27] A. Vaswani, N. Shazeer, N. Parmar, J. Uszkoreit, L. Jones, A. Gomez, L. Kaiser, and I. Polosukhin, "Attention is all you need," *Neural Information Processing Systems, Neural Information Processing Systems*, 2017.
- [28] X. Qian, W. Wang, L. Zhang, F. Zhu, Y. Fu, T. Xiang, Y.-G. Jiang, and X. Xue, "Long-term cloth-changing person re-identification," in *Proceedings of the Asian Conference on Computer Vision*, 2020.
- [29] P. Xu and X. Zhu, "Deepchange: A long-term person re-identification benchmark with clothes change," in *Proceedings of the IEEE/CVF International Conference on Computer Vision*, pp. 11196–11205, 2023.
- [30] X. Liu, K. Liu, J. Guo, P. Zhao, Y. Quan, and Q. Miao, "Pose-guided attention learning for cloth-changing person re-identification," *IEEE Transactions on Multimedia*, vol. 26, pp. 5490–5498, 2024.
- [31] L. Bao, L. Wei, W. Zhou, L. Liu, L. Xie, H. Li, and Q. Tian, "Multi-granularity matching transformer for text-based person search," *IEEE Transactions on Multimedia*, vol. 26, pp. 4281–4293, 2024.
- [32] Z. Wu, B. Ma, H. Chang, and S. Shan, "Refined knowledge transfer for language-based person search," *IEEE Transactions on Multimedia*, vol. 25, pp. 9315–9329, 2023.
- [33] J. Li, D. Li, C. Xiong, and S. Hoi, "Blip: Bootstrapping language-image pre-training for unified vision-language understanding and generation," in *International Conference on Machine Learning*, pp. 12888–12900, PMLR, 2022.
- [34] Y. Chen, G. Zhang, Y. Lu, Z. Wang, and Y. Zheng, "Tipcb: A simple but effective part-based convolutional baseline for text-based person search," *Neurocomputing*, vol. 494, pp. 171–181, 2022.
- [35] Z. Zheng, L. Zheng, M. Garrett, Y. Yang, M. Xu, and Y.-D. Shen, "Dual-path convolutional image-text embeddings with instance loss," *ACM Transactions on Multimedia Computing, Communications, and Applications (TOMM)*, vol. 16, no. 2, pp. 1–23, 2020.
- [36] Y. Zhang and H. Lu, "Deep cross-modal projection learning for image-text matching," in *Proceedings of the European conference on computer vision (ECCV)*, pp. 686–701, 2018.
- [37] Y. Wu, Z. Yan, X. Han, G. Li, C. Zou, and S. Cui, "Lapscore: language-guided person search via color reasoning," in *Proceedings of the IEEE/CVF International Conference on Computer Vision*, pp. 1624–1633, 2021.
- [38] D. Liu and H. Li, "Unleashing the imagination of text: A novel framework for text-to-image person retrieval via exploring the power of words," *arXiv preprint arXiv:2307.09059*, 2023.
- [39] Z. Wei, Z. Zhang, P. Wu, J. Wang, P. Wang, and Y. Zhang, "Fine-granularity alignment for text-based person retrieval via semantics-centric visual division," *IEEE Transactions on Circuits and Systems for Video Technology*, pp. 1–1, 2024.
- [40] S. Lee, D. Kim, and B. Han, "Cosmo: Content-style modulation for image retrieval with text feedback," in *2021 IEEE/CVF Conference on Computer Vision and Pattern Recognition (CVPR)*, 2021.
- [41] A. Agrawal, J. Lu, S. Antol, M. Mitchell, C. Zitnick, D. Batra, and D. Parikh, "Vqa: Visual question answering," *arXiv: Computation and Language, arXiv: Computation and Language*, 2015.
- [42] M. Cornia, M. Stefanini, L. Baraldi, and R. Cucchiara, "Meshed-memory transformer for image captioning," in *2020 IEEE/CVF Conference on Computer Vision and Pattern Recognition (CVPR)*, 2020.
- [43] X. Guo, H. Wu, Y. Cheng, S. Rennie, G. Tesauro, and R. Feris, "Dialog-based interactive image retrieval," *arXiv: Computer Vision and Pattern Recognition, arXiv: Computer Vision and Pattern Recognition*, 2018.
- [44] H. Wu, Y. Gao, X. Guo, Z. Al-Halah, S. Rennie, K. Grauman, and R. Feris, "Fashion iq: A new dataset towards retrieving images by natural language feedback," in *2021 IEEE/CVF Conference on Computer Vision and Pattern Recognition (CVPR)*, 2021.
- [45] Z. Liu, C. Rodriguez-Opazo, D. Teney, and S. Gould, "Image retrieval on real-life images with pre-trained vision-and-language models," in *2021 IEEE/CVF International Conference on Computer Vision (ICCV)*, 2021.
- [46] J. Devlin, M.-W. Chang, K. Lee, and K. Toutanova, "Bert: Pre-training of deep bidirectional transformers for language understanding," *arXiv preprint arXiv:1810.04805*, 2018.
- [47] K. Saito, K. Sohn, X. Zhang, C.-L. Li, C.-Y. Lee, K. Saenko, and T. Pfister, "Pic2word: Mapping pictures to words for zero-shot composed image retrieval," in *Proceedings of the IEEE/CVF Conference on Computer Vision and Pattern Recognition*, pp. 19305–19314, 2023.
- [48] A. Baldrati, L. Agnolucci, M. Bertini, and A. Del Bimbo, "Zero-shot composed image retrieval with textual inversion," *arXiv preprint arXiv:2303.15247*, 2023.
- [49] R. Gal, Y. Alaluf, Y. Atzmon, O. Patashnik, A. H. Bermano, G. Chechik, and D. Cohen-or, "An image is worth one word: Personalizing text-to-image generation using textual inversion," in *The Eleventh International Conference on Learning Representations*, 2022.
- [50] X. Gu, H. Chang, B. Ma, S. Bai, S. Shan, and X. Chen, "Clothes-changing person re-identification with rgb modality only," in *Proceedings of the IEEE/CVF Conference on Computer Vision and Pattern Recognition*, pp. 1060–1069, 2022.
- [51] L. Zheng, L. Shen, L. Tian, S. Wang, J. Wang, and Q. Tian, "Scalable person re-identification: A benchmark," in *Proceedings of the IEEE international conference on computer vision*, pp. 1116–1124, 2015.
- [52] L. Wei, S. Zhang, W. Gao, and Q. Tian, "Person transfer gan to bridge domain gap for person re-identification," in *Proceedings of the IEEE conference on computer vision and pattern recognition*, pp. 79–88, 2018.
- [53] W. Li and X. Wang, "Locally aligned feature transforms across views," in *Proceedings of the IEEE conference on computer vision and pattern recognition*, pp. 3594–3601, 2013.
- [54] W. Li, R. Zhao, T. Xiao, and X. Wang, "Deepreid: Deep filter pairing neural network for person re-identification," in *Proceedings of the IEEE conference on computer vision and pattern recognition*, pp. 152–159, 2014.
- [55] T. Xiao, S. Li, B. Wang, L. Lin, and X. Wang, "End-to-end deep learning for person search," *arXiv preprint arXiv:1604.01850*, vol. 2, no. 2, p. 4, 2016.
- [56] C. C. Loy, T. Xiang, and S. Gong, "Multi-camera activity correlation analysis," in *2009 IEEE Conference on Computer Vision and Pattern Recognition*, pp. 1988–1995, IEEE, 2009.
- [57] D. Gray and H. Tao, "Viewpoint invariant pedestrian recognition with an ensemble of localized features," in *Computer Vision–ECCV 2008: 10th European Conference on Computer Vision, Marseille, France, October 12–18, 2008, Proceedings, Part I 10*, pp. 262–275, Springer, 2008.
- [58] W. Zheng, "S, gong, and t," Xiang, "Associating groups of people," *BMVC*, 2009.
- [59] M. Hirzer, C. Beleznaï, P. M. Roth, and H. Bischof, "Person re-identification by descriptive and discriminative classification," in *Image Analysis: 17th Scandinavian Conference, SCIA 2011, Ystad, Sweden, May 2011. Proceedings 17*, pp. 91–102, Springer, 2011.
- [60] D. Kingma and J. Ba, "Adam: A method for stochastic optimization," *arXiv: Learning, arXiv: Learning*, 2014.
- [61] X. Qian, W. Wang, L. Zhang, F. Zhu, Y. Fu, T. Xiang, Y.-G. Jiang, and X. Xue, "Long-term cloth-changing person re-identification," in *Proceedings of the Asian Conference on Computer Vision*, 2020.
- [62] R. Sennrich, B. Haddow, and A. Birch, "Neural machine translation of rare words with subword units," *arXiv preprint arXiv:1508.07909*, 2015.